



FINAL REPORT

12 April 2021

For the project entitled:

Mapping Potential Desert Tortoise Habitat Connectivity in Clark County, NV

Submitted to:

Clark County

By:

Vincent A. Landau, MSc – Data Scientist

Miranda Gray, MSc – Lead Scientist

Brett G. Dickson, PhD – Chief Scientist

Introduction

The Mojave desert tortoise (*Gopherus agassizii*) is listed as “threatened” by the US Fish and Wildlife Service. A primary threat to their persistence is land cover/use change, which leads to habitat loss and fragmentation. Conserving habitat connectivity is important for maintaining genetic diversity and facilitating range shifts in response to climate change, and has emerged as a priority for desert tortoise management in Clark County. Connectivity models and associated maps for the desert tortoise have been developed recently (Gray et al. 2019), but to date landscape-scale movement and connectivity models have not directly incorporated terrain variables in a statistically robust way. Gray et al. (2019) were not able to model the impacts of terrain directly because tortoise movement data in and adjacent to rugged areas were not available at the time of their analysis. Instead, they accounted for the impacts of ruggedness by imposing a post hoc penalty on movement suitability as slope increased. The goal of the work detailed in this report was to develop an updated Mojave desert tortoise connectivity model that explicitly (and statistically) considered the impact of terrain on movement probability, and subsequently, habitat connectivity.

We used the same modeling approach as Gray et al. (2019), which itself used methods detailed in McClure et al. (2017). The modeling workflow had two primary steps: 1) generate a movement probability model to allow prediction, for each pixel in a rasterized representation of the landscape, of the relative probability that the pixel is suitable for movement, and 2) use the movement probability model to generate a “conductance surface,” in which each pixel is assigned a value proportional to the ease with which a tortoise could traverse it, and 3) use the conductance surface to model omni-directional landscape connectivity and generate a map of landscape connectivity. Each component of the workflow is described in detail in the methodology section of this report, but first, the theoretical framework upon which the connectivity modeling methods were built is described below.

Our methods were based on the circuit-theoretic landscape connectivity framework introduced by McRae (2006) and McRae et al. (2008). In this framework, the landscape is abstracted as a spatially referenced network of resistors, current sources, and grounds, with each component corresponding to a pixel in a raster representation of the landscape. The electrical current that flows through this electrical circuit corresponds to animal movement or other ecological flows (and in our case tortoises). The intensity and spatial arrangement of current flow is dictated by the spatial arrangement of the resistors, sources and ground. Current flow can be solved for using Ohm’s law and linear algebra (McRae et al. 2008), and the intensity of current for any given pixel is proportional to the probability that a random walker, traveling from the sources to the grounds, will pass through that pixel (McRae 2006). To make this approach to modeling connectivity more accessible, McRae and Shah (2008) created a software package called Circuitscape, which has since been updated and ported to the Julia programming language (Bezanson et al. 2017) as Circuitscape.jl (Anantharaman et al. 2020) to enable faster and more efficient computing (Anantharaman et al. 2020, Hall et al. 2021).

Most connectivity modeling studies to date have used a core-based approach, in which connectivity between discrete habitat patches (or cores) is modeled. Omni-directional (“coreless”) methods that preclude the need to delineate discrete cores are a more recent development (Anderson et al. 2012, Koen et al. 2014, Pelletier et al. 2014, McRae et al. 2016, Landau et al. 2021). These methods may be preferred in certain cases over core-based approaches for several reasons. First, results from core-based approaches can be highly sensitive to how and where cores are delineated (McRae et al. 2016). In landscapes that contain a full gradient of human modification and habitat suitability, delineation of cores can be subject to increasingly arbitrary decision points. Second, core-based approaches may not readily facilitate robust evaluation of connectivity within areas that would

otherwise be considered cores (McRae et al. 2016). Recently developed coreless approaches include wall-to-wall Circuitscape (Anderson et al. 2012) and Omniscape (McRae et al. 2016, Landau et al. 2021). Gray et al. (2019) made use of wall-to-wall Circuitscape, which we chose to similarly apply here.

Methods

The area of interest for this analysis was Clark County, Nevada. To reduce edge artifacts in the connectivity models, we extended the analysis region beyond the borders of Clark County by 15 km, then clipped that resulting region to the geographic range of the Mojave desert tortoise (Figure 1). To model omni-directional connectivity for the Mojave desert tortoise, we followed the methodology of Gray et al. (2019) in which relative movement probability (aka suitability) is modeled and used to parameterize resistance to movement for Circuitscape models (McClure et al. 2017). More specifically, our workflow included the following steps: 1) Compile and filter tortoise movement data and compute Brownian bridge movement models (BBMMs; Horne et al. 2007), 2) relate environmental covariates to BBMM values via regression, 3) predict movement suitability for the study area using regression results, 4) use the movement suitability prediction layer in combination with other data to create a “conductance” surface for input to Circuitscape, and 5) run wall-to-wall Circuitscape. Each of these steps are described below.

Movement data preparation and BBMMs

We used tortoise movement data from Gray et al. (2019) and Hromada et al. (2020). We removed data for 12 tortoises prior to model fitting. One tortoise was removed because it displayed strange movement patterns and was later found to have had a respiratory disease, and 11 other tortoises were removed because they were located along the fence lines of solar installations, so their movement was artificially restricted. In total, the final dataset included data for 135 tortoises across a total of eight different years (2008-2010 and 2016-2020). Tortoise locations from Hromada et al. (2020) were collected hourly, but data from Gray et al. (2019) were collected daily. To set all data to the same temporal scale, we filtered the data from Hromada et al (2020) to only retain the first relocation of each day for each tortoise. To retain only locations corresponding to movements that were likely occurring outside of burrow networks, which are the primary interest of this analysis, we further filtered the movement data to include only points that were at least 50 meters away from either the preceding or following points in the trajectory. Gray et al. (2019) used a shorter distance of 25 meters, but that was in part due to having access to a limited sample of movement data. Because we had access to a larger dataset, we increased the threshold to 50 meters in order to further tune the model toward the longer distance movements that may be more relevant and informative for landscape connectivity models. The final, filtered movement data used for model fitting are shown in Figure 1.

We calculated BBMMs for each tortoise within each year ($n = 293$ tortoise-year combinations) using the BBMM package (Neilson et al. 2013) in R (R Core Team 2020) to characterize the probability of a tortoise moving through a given pixel conditional on its movement data for a given year. BBMMs operate on the assumption of a random walk between each pair of successive animal locations. This assumption becomes less realistic as the time between relocations increases, so we only fit BBMMs between tortoise locations that were no greater than 24 hours apart.

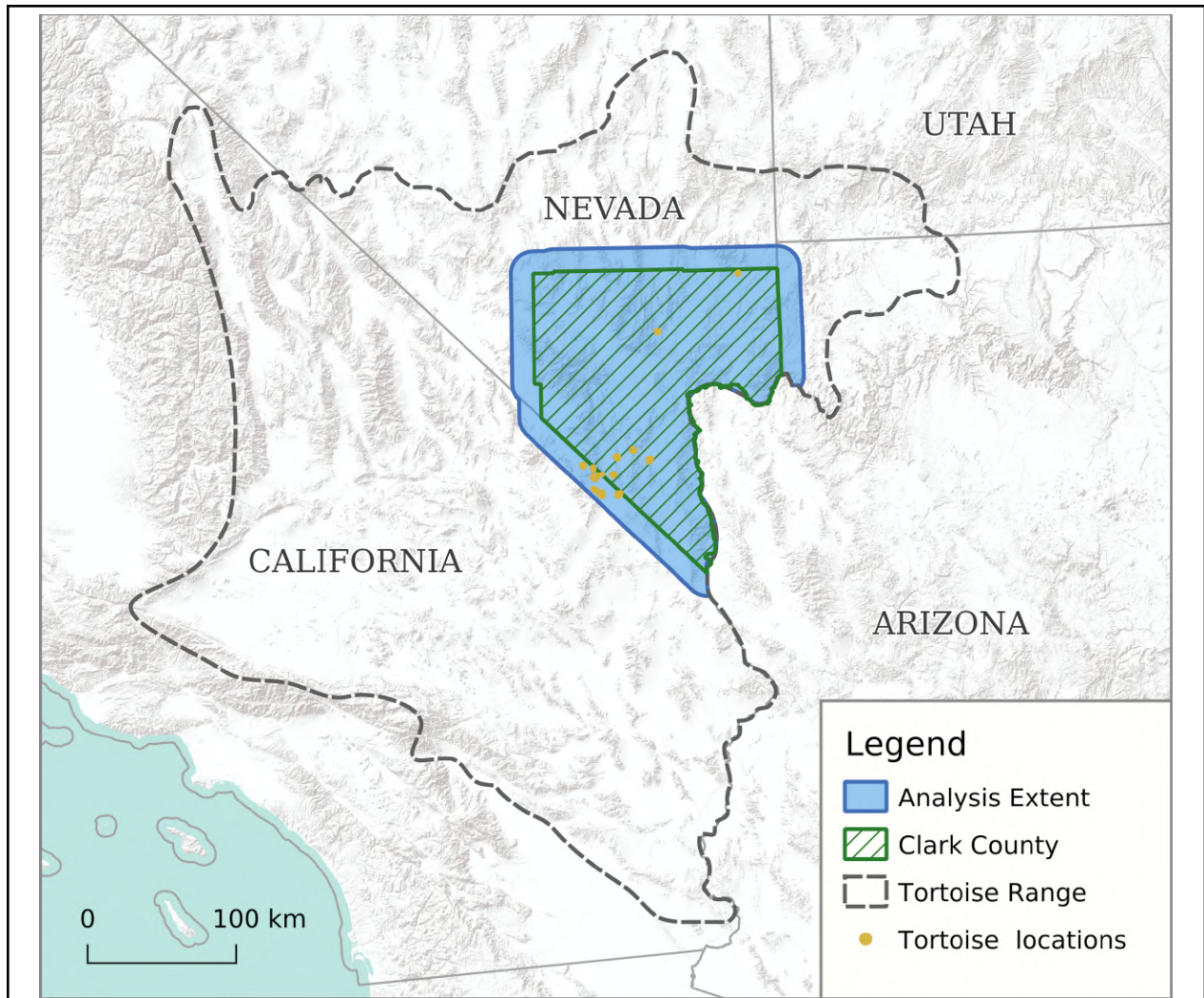


Figure 1 The analysis extent, Clark County, and the Mojave desert tortoise range. To generate the analysis extent, we buffered Clark County by 15 km, then clipped the resulting region with the Mojave desert tortoise range to exclude areas from the analysis where desert tortoises do not occur. We ran connectivity models for the bounding box of the analysis extent, and results provided in this report were clipped to Clark County to remove areas subject to artificial edge effects. The tortoise location data used for model fitting are overlaid.

Statistical movement suitability models

To model movement habitat suitability, we first collected a random spatial sample of 100 points in the footprint of each BBMM (one BBMM for each unique tortoise-year combination) to serve as the response variable in a regression model. Following Gray et al. (2019), we exclude pixels within BBMM rasters with values less than 1×10^{-8} , then we multiplied the BBMM surface by 1×10^8 to better facilitate model convergence. BBMM values against environmental covariates, following Gray et al. (2019). We used generalized linear mixed-effects models (GLMMs) with a log link function to relate BBMM response data to environmental covariates. Models incorporated a subject-level hierarchical random effect on the model intercept by year within tortoise ID. Models also used an exponential spatial covariance structure to account for residual spatial autocorrelation (Dormann et al. 2007). Model fitting was done in SAS Viya

(v3.4; ; SAS Institute, Cary, North Carolina, USA) via R. Models were fit and predictions were made at a 10-meter resolution.

Covariates

An objective of this analysis was to gain an improved understanding of the influence of terrain on tortoise movement. As such, we focused primarily on developing terrain covariates and relied on the literature to identify non-terrain variables of potential importance. We briefly describe the covariates we considered below, but further details on how each covariate was calculated can be found in Appendix A.

To characterize terrain, we considered three different covariates: the topographic position index (Dickson and Beier 2007), the vector ruggedness measure (Sappington et al. 2007), and slope. Using the vector ruggedness measure was particularly advantageous because it can be considered simultaneously with slope in any given model due to its low correlation with slope (Sappington et al. 2007). This is the primary reason that we favored VRM over other potential ruggedness metrics. We used the 30-meter resolution ALOS World 3D Digital Surface Model (Tadono et al. 2014) to compute all terrain variables. VRM can be considered for multiple neighborhood sizes. Because there was uncertainty around which neighborhood size would be most ecologically relevant and/or predictive of tortoise movement, we considered 3 different neighborhood sizes: 270 meters, 90 meters, and 8-nearest neighbors (a nine-pixel square window of 30x30 meter pixels centered on the target pixels). We found that only the 8-neighbor VRM had a correlation with slope less than 0.6, so the 8-neighbor variant advanced to the final modeling exercise and the others were dropped. TPI can also be considered for different neighborhood radii. We considered radii of 120 meters, 270 meters, and 1 km. Single variable models performed best with TPI at 1km so we used TPI at that scale; however, preliminary models that included TPI resulted in unrealistically high movement suitability in valleys (relative to non-valleys) so we dropped that covariate from consideration entirely in the final round of modeling.

The non-terrain covariates that we considered were the Normalized Difference Vegetation Index (NDVI; Rouse et al. 1974) (to approximate perennial vegetation), wash density (from Gray et al. 2019), mean daily maximum warm-season temperature (from Gray et al. 2019), and distance to the nearest minor road. In preliminary model runs, results suggested that sampling bias in the movement data was resulting in overfitting for mean daily maximum temperature. Additionally, models fit with distance to road as a covariate had ecologically unrealistic predictions (a decreasing movement probability with increasing distance from roads). As a result, we dropped distance to the nearest minor road and mean daily maximum temperature from consideration in the final round of modeling. All covariate rasters were standardized (to mean 0 and standard deviation 1) prior to model fitting.

Model selection and prediction averaging

We took an all-subsets approach to model selection in which we considered models for every possible combination of covariates. We also considered quadratic effects for NDVI and wash density. Models that included a quadratic effect were required to also include the linear term so that a true quadratic relationship was being modeled rather than a simple transformation of the covariate. We used the Akaike Information Criterion (AIC; Burnham and Anderson 2002) to evaluate model performance.

The primary objective of this modeling exercise was to generate good predictions (as opposed to inference) of desert tortoise movement for use in a connectivity model. Each covariate is represented by gridded spatial (raster) data. To generate “wall-to-wall” predictions of movement suitability for every pixel in the landscape, the covariate rasters can simply be combined according to the regression equation. For a single pixel, the predicted movement suitability can be calculated via a linear

combination of the pixel's covariate values (\mathbf{x}) and the model estimates of the regression coefficients (β) (Eq. 1).

$$\log(\hat{y}) = \mathbf{x}\beta \quad (1)$$

\hat{y} (Eq. 1) can be calculated by simply exponentiating the linear combination.

Model-averaged estimates of parameters (aka model-averaged betas) have been used commonly in the past in an attempt to make more robust predictions from regression models; however, using model-averaged regression coefficients is problematic and not advised when there is any degree of correlation between model covariates, which is almost always the case in practical regression modeling exercises (Cade 2015). As such, we instead opted to compute prediction rasters for each of the 10 best-performing models and combine them via a weighted mean (Equation 2). Taking the average of model *predictions* as opposed to computing a single prediction (for each pixel) using model-averaged betas is robust in the face of correlated covariates (Cade 2015). The weight for each model was set equal to its AIC weight, and weights were normalized to sum to one prior to computing the weighted mean. Final predictions for each pixel were calculated as the linear combination of a vector of model predictions (\mathbf{y}) for the top 10 models and a vector of their respective weights (\mathbf{w}), via the equation $\mathbf{w}\mathbf{y}$. We made predictions using this method for the entire bounding box of the analysis extent (Figure 1) to enable us to run wall-to-wall Circuitscape. Predictions of wash density were not available for a northwestern portion of Clark County because NAIP imagery was not available for that region (Gray et al. 2019). For the purpose of making predictions of movement suitability, we assumed a wash density value equal to the mean of the rest of the study area for any pixels for which predictions of wash density were not available (following Gray et al. 2019). We used the resulting movement suitability prediction surface as the foundation for a conductance surface to use in Circuitscape (described below).

Connectivity modeling

To model connectivity, we used Circuitscape and the wall-to-wall approach (Anderson et al. 2012). In the wall-to-wall approach, resistance (or conductance) is computed for a rectangular area (buffered to be larger than the focal area (to remove edge artifacts) and current is passed along the tile from east to west, and from south to north, then the current flow for each is summed to obtain a final map of connectivity. The resulting map depicts broad patterns in connectivity, and is particularly useful for identifying pinch points (areas where current flow is constricted, and therefore intensified).

This approach first requires the creation of a conductance surface that describes the ease (and likelihood) with which a tortoise could be expected to traverse a given pixel based on that pixel's attributes. We used the movement suitability surface generated from the regression model described above in combination with data for roads, urban development, land cover, solar energy facilities, wind turbines, and golf courses to create a resistance surface.

First, we rescaled the movement suitability surface from one to 100 (following Gray et al. 2019). We assigned a value of 1 (the minimum conductance, and maximum resistance) to developed pixels. A pixel was defined as developed if it was built-up or contained agriculture (NLCD classes 21-24, 81-82), fell inside the roads-removed Human Built-up and Settlement Database (HBASE; Wang et al. 2017), contained a primary road¹, fell in a golf course (manually digitized), contained solar development (manually digitized), or was within 450 meters of a wind turbine² (following Gray et al. (2019), using [FAA](#)

¹ For details on how primary and non-primary roads were defined, see Appendix B

² The study area contained only one wind turbine, and it fell within an otherwise developed area, so the inclusion of wind turbines likely did not affect connectivity model results

[Wind Turbine Location Data](#)). The addition to Interstate 11 northwest of Las Vegas was not included in the roads data we used, so we manually digitized it and considered it to be a primary road. We also assigned a conductance value of one to habitats that tortoises do not use, which included NLCD classes 11 (water), 41-43 (forest), and 90 and 95 (wetlands). For other land cover types and uses that likely impede tortoise movement to a lesser extent, we assigned a conductance value equal to the 10th percentile of the 1-100 rescaled movement suitability surface³ (following Gray et al. 2019). These land cover types included non-primary roads⁴, barren land (NLCD class 31), and areas with a particularly high NDVI (>0.25) thought to correspond to vegetation communities not used by desert tortoises. Finally, we entirely excluded areas with elevation greater than 2000 meters by setting those areas to NoData. The final conductance surface was resampled to a 30-meter resolution prior to running Circuitscape. We computed wall-to-wall omni-directional connectivity using Circuitscape.jl (Anatharaman et al. 2020) in the Julia programming language (Bezanson et al. 2017).

Model validation

To vet and validate our prediction of movement suitability for the desert tortoise, we undertook several exercises. First, we shared our movement suitability prediction surface with two leading Mojave desert tortoise experts for their evaluation, and second we used the Boyce Index (Boyce et al. 2002) to evaluate the performance of our model relative to the model from Gray et al. (2019). We computed the Boyce index using the movement data points used to fit the model. To evaluate the performance of our new model against the Gray et al. (2019) model, we compared the Boyce index for our movement suitability predictions to the Boyce index for the raw movement suitability predictions from Gray et al. (2019). We also compared the Boyce indices for our conductance surface versus Gray et al. (2019)'s conductance surface (which included a post-hoc correction for slope). Boyce indices were calculated using rank correlation and 10 bins. Finally, we qualitatively evaluated connectivity model predictions against out-of-sample tortoise location data that were collected from rugged areas.

Results

Movement suitability and conductance

The best-performing model included NDVI, slope, VRM, and wash density as covariates, with no quadratic effects; however, quadratic effects for both NDVI and wash density did appear as covariates among the 10 best-performing models (Table 1). The top model predicted a positive relationship for NDVI and wash density, which is in agreement with Gray et al. (2019), and a negative relationship for slope and VRM, as expected (Table 2). These relationships were consistent across the top 10 models (Table 2), and in models where quadratic relationships for NDVI or wash density were included, they were always concave down (Table 2). A concave down quadratic relationship means that a specific range of values of the covariate results in the highest movement suitability, and when values move further outside of that range (either higher or lower), movement suitability decreases. Predictions for the top 10 models (Table 1) were combined via weighted mean with weights proportional to their AIC weight to arrive at a final prediction surface for movement quality. Figure 2 shows the final, 1-100 scaled conductance surface.

³ If a pixel already had a movement suitability less than the 10th percentile, the original value was kept.

⁴ For details on how primary and non-primary roads were defined, see Appendix B

In general, higher movement suitability corresponded to regions with high perennial vegetation and washes that were not particularly steep or rugged (Figure 2). While slope and VRM had negative effects on movement suitability, moderately rugged areas still had reasonably high movement conductance, particularly when there was sufficient perennial vegetation cover. Across the top 10 models, NDVI consistently had the greatest influence on movement suitability (Table 2). VRM appeared in every one of the top 10 models, and was the only covariate to do so (Table 2).

Table 1. Model selection (AIC) results for the 10 best-performing models.

Model ID	Covariates	AIC	DELTA AIC	AIC Weight
1	NDVI, slope, VRM, wash density	87050.4	0.0	0.12
2	NDVI, slope, VRM	87050.7	0.3	0.10
3	slope, VRM	87051.8	1.4	0.06
4	NDVI, VRM, wash density	87051.8	1.4	0.06
5	slope, VRM, wash density	87051.8	1.4	0.06
6	NDVI, NDVI ² , slope, VRM, wash density	87052.2	1.8	0.05
7	NDVI, slope, VRM, wash density, wash density ²	87052.3	1.9	0.05
8	NDVI, VRM	87052.4	2.0	0.04
9	NDVI, NDVI ² , slope, VRM	87052.5	2.1	0.04
10	VRM, wash density	87053.1	2.7	0.03

Table 2 Parameter estimates (mean and standard error) for the 10 best-performing models. For a given model, dashes are placed under covariates that were not considered in that model. See Appendix A for a full description of model covariates.

Model Rank	Intercept		NDVI		NDVI Squared		Wash Density		Wash Density Squared		Slope		VRM	
	Mean	SE	Mean	SE	Mean	SE	Mean	SE	Mean	SE	Mean	SE	Mean	SE
1	-1.086	0.152	0.048	0.021	--	--	0.008	0.003	--	--	-0.037	0.018	-0.033	0.015
2	-1.086	0.152	0.047	0.022	--	--	--	--	--	--	-0.040	0.018	-0.033	0.015
3	-1.100	0.153	--	--	--	--	--	--	--	--	-0.040	0.018	-0.032	0.015
4	-1.072	0.152	0.048	0.021	--	--	0.009	0.003	--	--	--	--	-0.028	0.015
5	-1.100	0.153	--	--	--	--	0.008	0.003	--	--	-0.037	0.018	-0.032	0.015
6	-1.082	0.152	0.060	0.025	-0.005	0.006	0.008	0.003	--	--	-0.037	0.018	-0.033	0.015
7	-1.086	0.152	0.049	0.021	--	--	0.005	0.005	0.001	0.001	-0.038	0.018	-0.003	0.015
8	-1.071	0.152	0.047	0.021	--	--	--	--	--	--	--	--	-0.028	0.015
9	-1.082	0.152	0.058	0.025	-0.005	0.006	--	--	--	--	-0.040	0.018	-0.033	0.015
10	-1.086	0.153	--	--	--	--	0.008	0.003	--	--	--	--	-0.028	0.015

Validation

Two external Mojave desert tortoise experts were in agreement that our movement suitability predictions were generally reasonable given their understanding of tortoise ecology. One potential problem area that was flagged by the experts was the region of high movement suitability between the Lucy Gray mountains and McCullough mountain, a region where they have not observed desert

tortoises. The model from Gray et al. (2019) shows similar predictions for the eastern section of this region, but predictions by our model are higher on the lower-elevation section of the western slope of McCullough mountain.

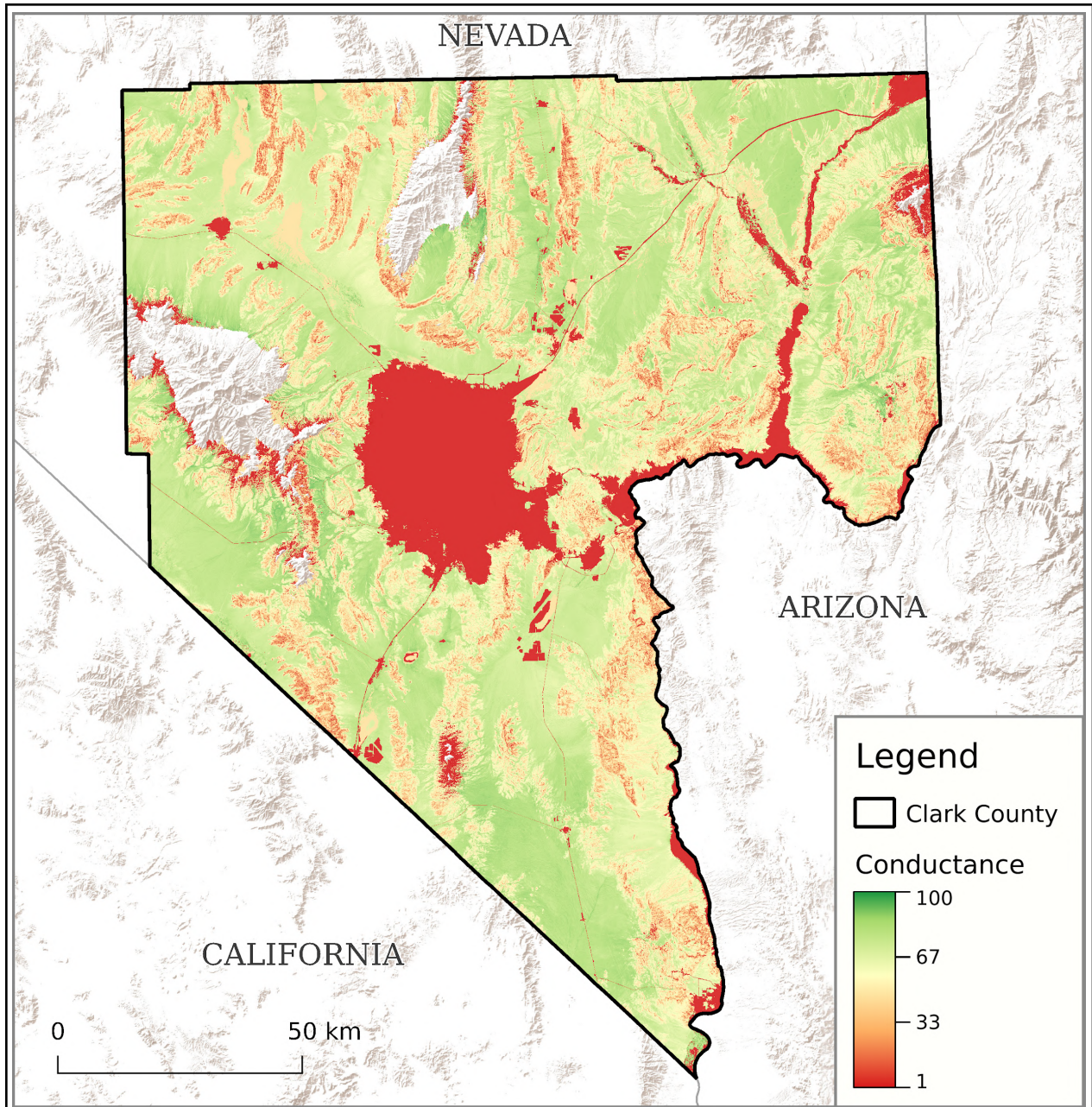


Figure 2 The conductance surface (clipped to Clark County) that was used as input to Circuitscape. Conductance was primarily based on our movement suitability prediction, but included post hoc alterations to account for land cover and use types that we could not directly incorporate into the modeling process, including major roads, urban development, solar development, golf courses, and NLCD land cover class.

Our movement suitability model performed much better than the raw movement suitability from Gray et al. (2019). Our model had a Boyce index of 0.73 suggesting a reasonable model fit, compared to a value of 0.115 for Gray et al. (2019), suggesting a very poor model fit. Since these raw

outputs were not what was ultimately used with Circuitscape in either our case or in Gray et al. (2019), we also compared the Boyce indices for conductance surfaces. Our conductance surface performed well with a value of 0.854. The conductance surface from Gray et al. (2019) performed similarly well, with a value of 0.891.

Connectivity Modeling

Wall-to-wall current flow from Circuitscape is shown in Figure 3. Connectivity is most constrained around Las Vegas, which serves to divert and intensify desert tortoise movement. In general, predicted movement intensity is consistently high in southern Clark County. In northeast and northwest Clark County, current flow is moderate to low despite high conductance values in those regions. This suggests that these regions may have more path redundancy than the rest of the county.

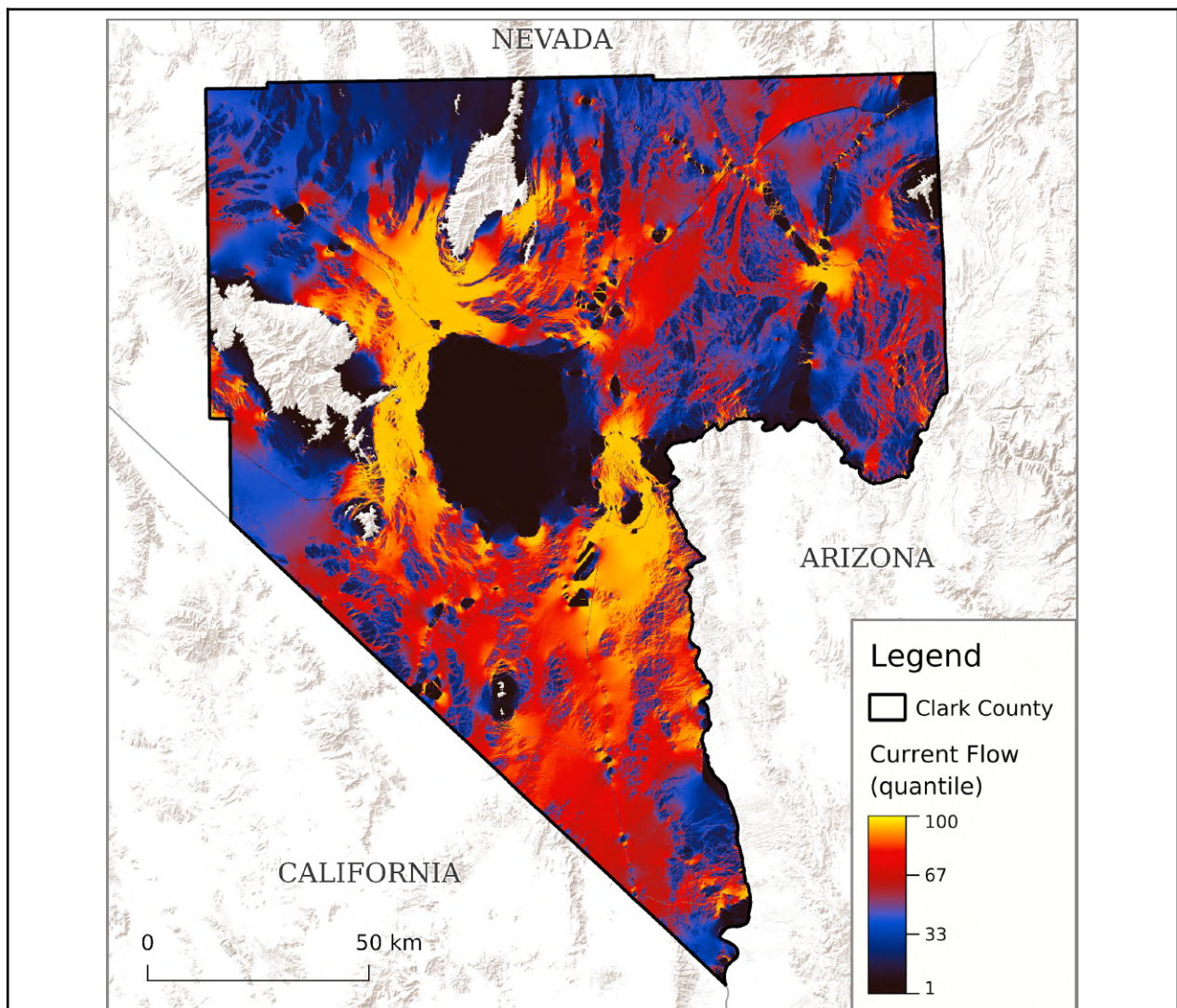
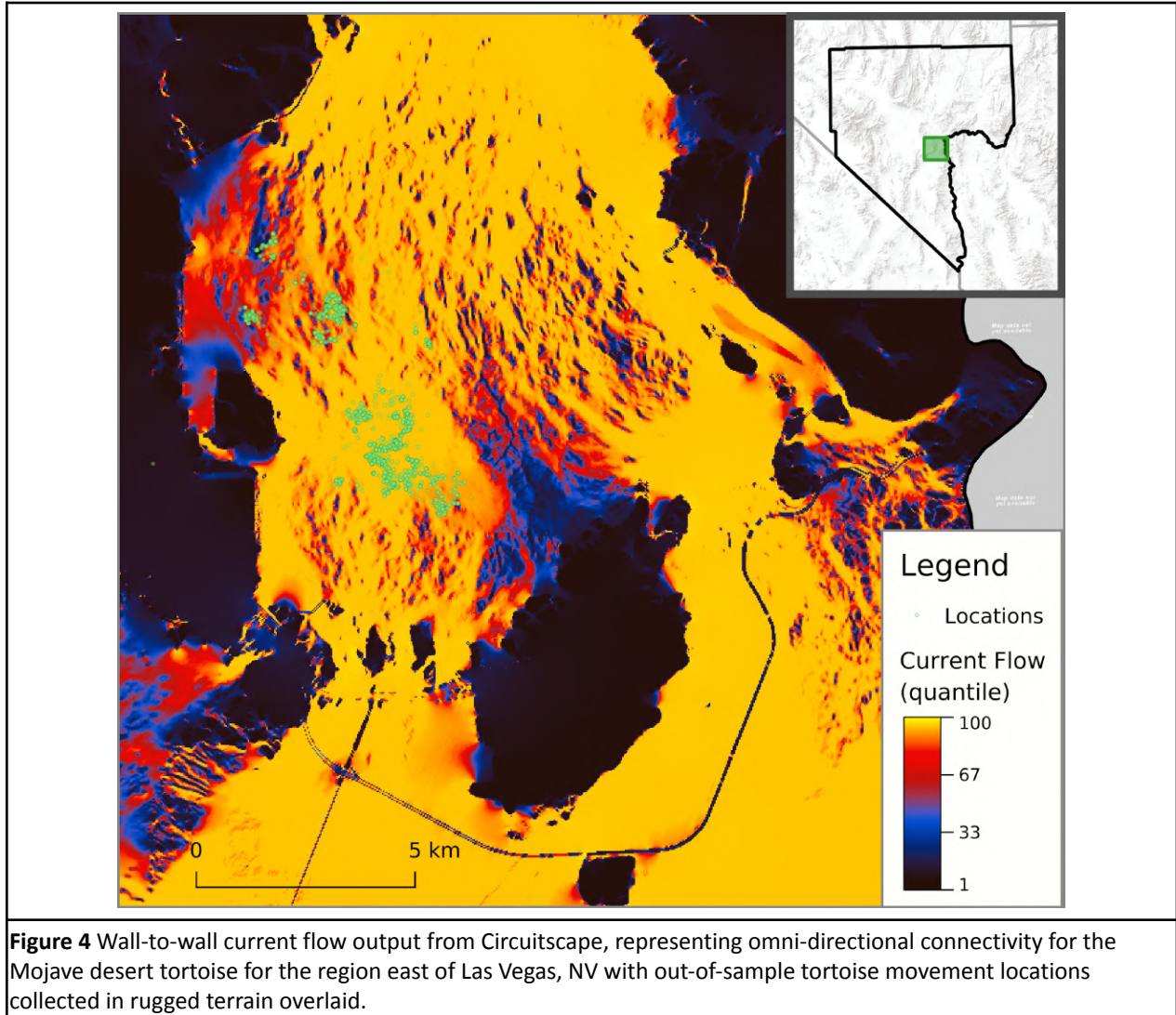


Figure 3 Omni-directional connectivity output from Circuitscape for the Mojave desert tortoise in Clark County, NV. Current flow was visualized using a quantile color ramp with 20 breaks. A higher value indicates a higher amount of predicted movement and/or gene flow.

In general, current flow predictions were also in agreement with out-of-sample tortoise movement data collected from rugged areas. An example is shown in Figure 2.



Discussion

Interpreting the connectivity map must be done with care. Current flow values are related to the intensity with which tortoises are expected to move through any given pixel. If a pixel has a low current flow value, it does not directly mean that the pixel is a barrier to movement, it simply means that less tortoises are expected to traverse it. This *could* be because that pixel has characteristics that cause it to act as a barrier (or similarly if the pixel is surrounded on all sides by barriers), but it may be because there is a “better” path nearby, or because there are many potential suitable paths (path redundancy), thus preventing movement from being channelized. This is likely the case in the northeast and northwest portions of Clark County, as these areas have high conductance, but low current flow. When a pixel has a high current flow value relative to the rest of the landscape, it means that more movement is expected to flow through that pixel. In the wall-to-wall Circuitscape case, high current flow results as a

consequence of areas of low conductance (high resistance) channelizing movement into adjacent narrow pathways that have higher conductance. These high current areas, referred to as “pinch points” (McRae et al. 2008), can be considered high priority for maintaining the overall connectivity of the entire landscape and as such, should be a focus of connectivity conservation efforts (Dickson et al. 2013).

While our results perform well according to our validation exercises, it is important to note that the data used for model fitting were biased in geographic space (Figure 1). A bias in geographic space may mean that there is a bias in the covariate space as well, and we expect this to be the case given the spatial distribution of the movement data used to fit the model. This sort of bias was evident for both temperature and distance-to-road covariates that we considered in the early phases of this analysis. Because location data were biased and did not fully cover the range of suitable values in temperature and distance to road, we were not able to include those covariates.

As a result of this analysis, several potential priorities for future research have emerged. First and foremost, it will be critically important to validate these model results in the field. Additional monitoring, particularly in the highest current flow areas, should be done to evaluate how predictive our model is of tortoise movement and/or occurrence in reality. The collection of more tortoise movement data across Clark county also emerges as a priority for future research, both for validation of existing models, and for use in future movement and connectivity modeling. In particular, collecting data across a larger gradient of terrain, vegetation, and climate characteristics would serve to improve inference in future models. Data have been collected in rugged areas (e.g., see Figure 4), but these data were not collected at a high enough temporal resolution to be useful for Brownian bridge movement modeling. For future data to be useful for Brownian bridge movement modeling, it is critical that they are collected frequently enough. Ideally, relocations should be obtained at least every 24 hours.

Our movement suitability model (Figure 2) represents a step toward more fully understanding how terrain affects tortoise movement. The conductance surface used in Gray et al. (2019) performed similarly based on the Boyce index; however, because our model did not need to rely on post-hoc corrections for slope due to increased data availability, our results serve to provide additional support for the accuracy of the final connectivity model from Gray et al. (2019), in addition to providing quantitative estimates of the influence of slope and terrain ruggedness (VRM) on tortoise movement. VRM appeared in every one of the top 10 models, suggesting that it may be particularly valuable for predicting tortoise movement suitability. Our connectivity map highlights the areas that, based on the data and covariates used to fit our movement suitability model, are most important for maintaining overall connectivity for Mojave desert tortoises in Clark County, NV. Upon field validation of our connectivity model, these areas should be the focus of conservation efforts moving forward.

Literature cited

- Anantharaman, R., Hall, K., Shah, V. and Edelman, A., 2020. Circuitscape in Julia: High Performance Connectivity Modelling to Support Conservation Decisions. *JuliaCon Proceedings*, 1(1), 58, <https://doi.org/10.21105/jcon.00058>
- Anderson, M.G., Barnett, A., Clark, M., Prince, J., Olivero Sheldon, A. and Vickery, B., 2016. Resilient and connected landscapes for terrestrial conservation. *The Nature Conservancy, Eastern Conservation Science, Eastern Regional Office Boston, MA*, 1-149. Available online: <https://www.nature.ly/TNCResilience>
- Burnham, K. P., and D. R. Anderson. 2002. Model selection and multimodel inference: a practical information theoretic approach. Second edition. *Springer, New York, New York, USA*.
- Dickson, B.G., Roemer, G.W., McRae, B.H. and Rundall, J.M., 2013. Models of regional habitat quality and connectivity for pumas (*Puma concolor*) in the southwestern United States. *PLoS one*, 8(12), p.e81898.
- Gray, M.E., Dickson, B.G., Nussear, K.E., Esque, T.C. and Chang, T., 2019. A range-wide model of contemporary, omnidirectional connectivity for the threatened Mojave desert tortoise. *Ecosphere*, 10(9), e02847.
- Bezanson, J., Edelman, A., Karpinski, S. and Shah, V.B., 2017. Julia: A fresh approach to numerical computing. *SIAM review*, 59(1), 65-98.
- Cade, B.S., 2015. Model averaging and muddled multimodel inferences. *Ecology*, 96(9), 2370-2382.
- Dickson, B.G. and Beier, P., 2007. Quantifying the influence of topographic position on cougar (*Puma concolor*) movement in southern California, USA. *Journal of Zoology*, 271(3), pp.270-277.
- Dormann, C.F., McPherson, J.M., Araújo, M.B., Bivand, R., Bolliger, J., Carl, G., Davies, R.G., Hirzel, A., Jetz, W., Kissling, D.W. and Kühn, I., 2007. Methods to account for spatial autocorrelation in the analysis of species distributional data: a review. *Ecography*, 30(5), 609-628.
- Hall, K.R., Anantharaman, R., Landau, V.A., Clark, M., Dickson, B.G., Jones, A., Platt, J., Edelman, A. and Shah, V.B., 2021. Circuitscape in Julia: Empowering Dynamic Approaches to Connectivity Assessment. *Land*, 10(3), p.301.
- Horne, J.S., Garton, E.O., Krone, S.M. and Lewis, J.S., 2007. Analyzing animal movements using Brownian bridges. *Ecology*, 88(9), 2354-2363.
- Hromada, S.J., Esque, T.C., Vandergast, A.G., Dutcher, K.E., Mitchell, C.I., Gray, M.E., Chang, T., Dickson, B.G. and Nussear, K.E., 2020. Using movement to inform conservation corridor design for Mojave desert tortoise. *Movement Ecology*, 8(1), 1-18.
- Koen, E.L., Bowman, J., Sadowski, C. and Walpole, A.A., 2014. Landscape connectivity for wildlife: development and validation of multispecies linkage maps. *Methods in Ecology and Evolution*, 5(7), 626-633.
- Landau, V.A., Shah, V.B., Anantharaman, R. and Hall, K.R., 2021. Omniscape. jl: Software to compute omnidirectional landscape connectivity. *Journal of Open Source Software*, 6(57), 2829.
- McClure, M.L., Dickson, B.G. and Nicholson, K.L., 2017. Modeling connectivity to identify current and future anthropogenic barriers to movement of large carnivores: a case study in the American Southwest. *Ecology and Evolution*, 7(11), 3762-3772.
- McRae, B.H., 2006. Isolation by resistance. *Evolution*, 60(8), 1551-1561.
- McRae, B.H., Dickson, B.G., Keitt, T.H. and Shah, V.B., 2008. Using circuit theory to model connectivity in ecology, evolution, and conservation. *Ecology*, 89(10), 2712-2724.

- McRae, B.H., Popper, K., Jones, A., Schindel, M., Buttrick, S., Hall, K., Unnasch, R.S. and Platt, J., 2016. Conserving nature's stage: mapping omnidirectional connectivity for resilient terrestrial landscapes in the pacific northwest. *The Nature Conservancy, Portland, Oregon*.
- Nielson, R.M., Sawyer, H. and McDonald, T.L., 2013. BBMM: Brownian bridge movement model. *R package version, 3*.
- Pelletier, D., Clark, M., Anderson, M.G., Rayfield, B., Wulder, M.A. and Cardille, J.A., 2014. Applying circuit theory for corridor expansion and management at regional scales: tiling, pinch points, and omnidirectional connectivity. *PLoS One, 9*(1), e84135.
- R Core Team, 2020. R: A language and environment for statistical computing. R Foundation for Statistical Computing, Vienna, Austria. <https://www.R-project.org/>.
- Rouse, J.W., Haas, R.H., Schell, J.A. and Deering, D.W., 1974. Monitoring vegetation systems in the Great Plains with ERTS. *NASA special publication, 351*(1974), 309.
- Sappington, J.M., Longshore, K.M. and Thompson, D.B., 2007. Quantifying landscape ruggedness for animal habitat analysis: a case study using bighorn sheep in the Mojave Desert. *The Journal of wildlife management, 71*(5), 1419-1426.
- Tadono, T., Ishida, H., Oda, F., Naito, S., Minakawa, K. and Iwamoto, H., 2014. Precise global DEM generation by ALOS PRISM. *ISPRS Annals of the Photogrammetry, Remote Sensing and Spatial Information Sciences, 2*(4), 71.
- Wang, P., Huang, C., Brown de Colstoun, E.C., Tilton, J.C. and Tan, B., 2017. Documentation for the global human built-up and settlement extent (HBASE) dataset from Landsat. *Palisades, NY: NASA Socioeconomic Data and Applications Center (SEDAC)*. <https://doi.org/10.7927/H4DN434S>.

Appendix A

Covariate calculation

All covariates were computed using Google Earth Engine (Gorelick et al. 2017). For terrain variables, we used the 30-meter resolution ALOS World 3D Digital Surface Model (Tadono et al. 2014). While 10-meter resolution elevation data were available for the study area from the United States National Elevation Dataset (US NED), we opted instead to use the ALOS DSM because it is much less subject to the striping artifacts and inaccuracies seen in the US NED. When needed, covariates were resampled to 10-meter resolution via bilinear interpolation prior to model fitting and prediction.

Topographic Position Index

The Topographic Position Index (TPI; Dickson and Beier 2007) measures the degree to which each pixel's elevation differs the mean elevation in its neighborhood. The TPI for a given pixel is calculated as

$$\text{TPI} = e - \text{mean}(\mathbf{e}_n)$$

where e is the elevation of the pixel, and \mathbf{e}_n is a vector of the elevation values within a neighborhood centered on the pixel. We used a circular neighborhood for the purposes of identifying and averaging neighborhood pixels, and considered multiple scales of 120, 250, and 1000 meters. We additionally considered the TPI z-score (TPI_z), where the TPI for a given pixel is standardized based on the standard deviation of elevation within the neighborhood:

$$\text{TPI}_z = (e - \text{mean}(\mathbf{e}_n)) / \text{sd}(\mathbf{e}_n)$$

In addition to the single scale TPI measurements, we also considered multiscale variants, calculated as the average of the TPI or TPI_z values, at the 120, 250, and 1000 meter scales. TPI at 1km performed best, according to AIC in single-variable models, so that version was used in final modeling; however, preliminary models that included TPI resulted in unrealistically high movement suitability in valleys (relative to non-valleys) so we dropped that covariate from consideration entirely in the final round of modeling.

Vector Ruggedness Measure

The Vector Ruggedness Measure (VRM; Sappington 2007) offers a way to measure topographic complexity and variability. The VRM differs from other ruggedness metrics in that it does a good job of maintaining relative independence from slope. In order for a pixel to have a high VRM, it must have both steep slopes *and* variation in aspect within its neighborhood. Sloping hillsides that are flat but inclined do not receive high VRM values. To start, we calculated VRM using a 3x3 square of pixels as the neighborhood, which is typically the neighborhood used to measure VRM (Sappington et al. 2007). However, VRM can be calculated for larger windows as well, as described in Sappington et al. (2007), so we additionally considered radii of 90 meters and 270 meters to explore the potential effects of

ruggedness at larger scales. Because this metric is generally uncorrelated with slope, the two can be included in the same model, and the effects of each can be isolated. However, when considering the larger radii, we found the VRM became increasingly correlated with slope, so we considered only the 3x3 neighborhood (8-neighbor) variant of VRM because understanding the influence of slope was of interest given our project objectives.

Slope

Slope was calculated using the built-in `ee.Terrain.slope()` method in Google Earth Engine (Gorelick 2017).

Normalized Difference Vegetation Index (NDVI)

Perennial vegetation is an important limiting factor for tortoise habitat use and movement, because it offers protection from solar radiation as well as food resources during the duration of the non-hibernating season (Gray et al. 2019). We characterized perennial vegetation using the Normalized Difference Vegetation Index (NDVI; Rouse et al. 1974) from Sentinel 2A satellite imagery products (European Space Agency, Drusch et al. 2012). For each landscape pixel in the study area, we computed the median NDVI value for all Sentinel 2A images dating between June 15th 2019 and August 31st 2019. June 15th to August 31st is the time period when annual vegetation is at its lowest, and 2019 in particular was a drier year for the study area, so any NDVI signal during that time period can be reasonably attributed to perennial vegetation. Sentinel 2A images for the time period that was summarized were sufficiently cloud-free, so cloud masking was not needed. We additionally considered moving window averages of NDVI with a 30 meter and 90 meter radius. In single-variable models, NDVI at 10 meters resolution (no moving window averaging) performed best, so that scale advanced forward and others were dropped.

Average Maximum Temperature of the Warmest month

Following Gray et al. (2019), we included a covariate describing the average maximum temperature of the warmest month (see Gray et al. 2019 for a description of how the layer was derived); however, in preliminary model runs, we found that the model was extremely overfit such that only a narrow range of temperatures resulted in high movement suitability. During an evaluation of preliminary model results, experts agreed that the predicted relationship between tortoise movement suitability and temperature was overfit and ecologically unrealistic, and it was likely a result of sampling bias. We excluded this covariate from consideration in our final round of modeling.

Distance to Minor Road

We included distance to minor roads as a covariate following Gray et al. (2019). To characterize minor roads, we used the TIGER roads database for 2019 and retained features with MTFCC codes of 'S1400' (Local Neighborhood Road, Rural Road, City Street) and 'S1500' (Vehicular Trail-4WD), then calculated for every 10-meter pixel the distance to the nearest minor road. Preliminary model runs yield nonsensical results (a negative correlation between distance to road and movement suitability) so we dropped it from consideration in our final models.

Wash Density

Desert washes have been recognized as an important predictor of desert tortoise space use (Gray et al. 2019). We used the wash classification model generated by Gray et al. (2019), who originally calculated

the probability that a given pixel is a wash at a 1-meter resolution. We reduced the resolution of the raster data to a 10-meters, and calculated wash density as the average wash probability of the 1 meter pixels that fell within each 10-meter pixel. This resulted in a prediction for each 10-meter pixel of the expected proportion of 1 meter pixels within it that would be classified as a wash. We further improved the accuracy of the original wash layer by setting wash probabilities to zero for any pixels that fell within a road (based on TIGER road data), had a slope greater than 15 degrees, or were human modified (HM>0.4, based on human modification data from Conservation Science Partners (2019)).

Literature cited

- Conservation Science Partners (CSP). 2019. Methods and approach used to estimate the loss and fragmentation of natural lands in the conterminous U.S. from 2001 to 2017. *Technical Report. Truckee, CA.*
- Dickson, B.G. and Beier, P., 2007. Quantifying the influence of topographic position on cougar (*Puma concolor*) movement in southern California, USA. *Journal of Zoology*, 271(3), pp.270-277.
- Drusch, M., Del Bello, U., Carlier, S., Colin, O., Fernandez, V., Gascon, F., Hoersch, B., Isola, C., Laberinti, P., Martimort, P. and Meygret, A., 2012. Sentinel-2: ESA's optical high-resolution mission for GMES operational services. *Remote sensing of Environment*, 120, 25-36.
- Gorelick, N., Hancher, M., Dixon, M., Ilyushchenko, S., Thau, D. and Moore, R., 2017. Google Earth Engine: Planetary-scale geospatial analysis for everyone. *Remote sensing of Environment*, 202, 18-27.
- Tadono, T., Ishida, H., Oda, F., Naito, S., Minakawa, K. and Iwamoto, H., 2014. Precise global DEM generation by ALOS PRISM. *ISPRS Annals of the Photogrammetry, Remote Sensing and Spatial Information Sciences*, 2(4), 71.
- Sappington, J.M., Longshore, K.M. and Thompson, D.B., 2007. Quantifying landscape ruggedness for animal habitat analysis: a case study using bighorn sheep in the Mojave Desert. *The Journal of wildlife management*, 71(5), 1419-1426.

Appendix B

Road classification

We used TIGER road data for 2016 for consistency with Gray et al. (2019) and because there were not significant changes to major non-dirt roads since 2016, other than the Interstate 11 extension northwest of Las Vegas, which we manually digitized. We followed the same procedure as Gray et al. (2019) for assigning roads to primary and non-primary categories. First, we filtered the TIGER roads data to only retain roads of type (rttype) 'C', 'I', 'M', 'S', or 'U'.

Primary roads were defined as roads with an MTFCC class of 'S1100', 'S1200', or 'S1630'. This classification resulted in the inclusion of a dirt section of State Highway 16, which was likely misclassified in the TIGER roads database. We manually removed that road from the primary roads category and placed it in the non-primary roads category.

Non-primary roads were identified as roads with an MTFCC class not equal to 'S1100', 'S1200', or 'S1630'. This condition resulted in the inclusion of many very minor dirt roads that likely do not have a significant influence on tortoise movement. In collaboration with tortoise experts, Gray et al. (2019) identified a list of roads to exclude from the non-primary road category. We similarly excluded these roads in our analysis. The following roads (based on the TIGER "FULLNAME" attribute) were removed:

```
'Stateline Rd', 'Old Spanish Hwy', 'Co Rd 20913', 'Wagon  
Springs Rd', 'Slate Mine Rd', 'Coloseum Rd', 'Kingston Rd',  
'Rainbow Quarry Rd', 'Reimann Rd', 'Cabin Springs Rd', 'Alamo  
Rd', 'Wamp Springs Trl', 'Gunsight Mountain Trl', 'Dry Gulch',  
'Smith Talc Rd', 'Mesquite-Valley', 'Dead Horse Trl', 'Pine  
Canyon Rd', 'Hidden Forest Rd', 'Cow Camp Rd', 'Yates Well Rd',  
'Greens Well Rd', 'County 20913 Rd', 'Nमित Rd', 'County 20545  
Rd', 'Greenwater Valley Rd', 'Lost Section Rd', 'Lost Section  
Rd S', 'Dantes View Rd', "Dante's View Rd", 'Gas Pipeline Rd',  
'Nps 30', 'Furnace Creek Rd', 'Furnace Creek Wash Rd', 'Green  
Water Valley Rd', 'Western Talc Rd', 'Excelsior Mine Rd', 'Bell  
Vista Ave', 'White Rock Rd', 'Death Valley National Park', 'Old  
Corn Creek Rd', 'Mesquite Valley Rd', 'W Extension, Bell Vista  
Rd', 'W Extension Irene St', 'Pahrump Valley Blvd Exd'
```